PHYSICAL REVIEW E, VOLUME 63, 050201(R)

Density functional theory for colloidal rod-sphere mixtures

Matthias Schmidt
Institut für Theoretische Physik II, Heinrich-Heine-Universität Düsseldorf, Universitätsstraße 1, D-40225 Düsseldorf, Germany
(Received 13 December 2000; published 11 April 2001)

We present a density functional theory for a model colloidal mixture of hard spheres and infinitely thin hard rods. For these freely rotating particles, we use a fundamental measures approach to obtain a functional that features the correct dimensional crossover and the exact low density limit. For isotropic bulk fluid mixtures, the free energy, and hence the demixing phase diagram, are identical to that obtained from free volume theory. Results for the partial pair correlation functions of the bulk mixture are in good agreement with those of our simulations.

DOI: 10.1103/PhysRevE.63.050201 PACS number(s): 61.20.Gy, 61.30.Cz, 64.70.Ja, 82.70.Dd

Colloidal mixtures of differently shaped or sized particles serve as well-defined model systems for the study of a wide range of phenomena in condensed matter. These include structural correlations, demixing phase transitions, and freezing. Such systems can be prepared so that they possess primarily hard body pair interactions; hence, entropy plays the dominant role. Creating binary mixtures by adding a second component to monodisperse colloidal hard spheres (HS) provides the work horse in the field. Among the various different second components are smaller-sized spherical particles, leading to binary hard sphere mixtures [1], globular nonadsorbing polymers [2], and rodlike colloids [3,4] or polymers. In these situations, the additive is often regarded as an agent that mediates an effective interaction between the spheres by means of the depletion mechanism. For rods considerable recent work was done to reveal the nature of the depletion [5,6]. The benefit of this approach is the analogy to simple substances possessing an attractive pair potential. However, the depletant's degrees of freedom are no longer accessible, and, in general, effective many-body interactions between the spheres occur, which are difficult to treat. Both drawbacks can be circumvented by treating the full binary mixture, without any explicit integrating-out procedure.

A simple rod-sphere model was introduced by Bolhuis and Frenkel (BF) [7]. It consists of a mixture of hard spheres and hard, infinitely thin rods (needles). The needle volume, and hence the interaction between needles, vanishes in this limit. Clearly, this is a gross simplification. However, rod aspect ratios can be as high as 25 in experiments with silica coated boehmite rods [4] mixed with silica spheres, and the rod densities are typically well below the Onsager nematic-isotropic transition [4]. BF's model can be thought of as the simplest in the present context, playing a role similar to the Asakura-Oosawa (AO) model [2] for the case of spherical colloids and added polymer. BF's computer simulations showed that the model undergoes a demixing transition into sphere-rich (rod-poor) and sphere-poor (rod-rich) phases. They also extended Lekkerkerker's free volume theory [8] for the AO model to their case. Comparing with simulation results for the binodals, they found that '' . . . the accuracy of the theoretical curves is surprising'' [7]. Subsequently, finite rod thickness could also be treated [3]. Little attention, however, has been payed to the model's bulk structural correlations, to its behavior in inhomogeneous situations, as, for example, induced by walls, or to the free interface between demixed phases.

In this work, we present a density-functional theory (DFT) [9] for the binary needle-sphere mixture that allows us to study correlations in bulk as well as in arbitrary inhomogeneous situations. It is based on Rosenfeld's fundamental measures theory [10,11] and Tarazona's latest extension to this [12], ensuring that local packing effects are correctly included. The free energy of the homogeneous fluid, and hence, the demixing curve, are the same as in BF's free volume theory. Our DFT features the correct virial expansion. In the literature it has been stated by several authors [11,13,14], that an impossibility of deconvolution of the Mayer function for *arbitrary* convex bodies prohibits this sort of geometrically based DFT. Here we give an explicit counterexample; albeit dealing with a model where interactions between rods are absent, we present the first such theory for freely rotating anisotropic particles. Our functional has the correct dimensional crossover to situations of reduced spatial dimensionality, an important property that only recently was achieved for one-component hard spheres [12]. As an application, we reconsider the phase diagram and then focus on the bulk pair correlations in the sphere-needle mixture where we find good agreement between the DFT results and our computer simulations.

Let us first describe the needle-sphere model. We consider a mixture of hard spheres (species S) with radii R, and infinitely thin needles (species N) with length L, and number densities ρ_S and ρ_N, respectively. The pair interaction between spheres is $V_{SS}=\infty$ if the separation between sphere centers is less than $2R$, and zero otherwise; the pair interaction between a sphere and a needle is $V_{SN}=\infty$, if both overlap, and zero else; the interaction between needles vanishes for all separations, $V_{NN}=0$. We denote the sphere diameter by $\sigma=2R$, and the sphere packing fraction by $\eta=4\pi R^3\rho_S/3$. In Fig. 1 a snapshot from computer simulation (described below) is shown to illustrate the model.

In order to construct the DFT, we start with a geometrical representation of the particles in terms of weight functions w_μ^i, where i labels the species, and $\mu=3,2,1$, and 0 corresponds to the particles' volume, surface, integral mean curvature, and Euler characteristic, respectively [11]. The weight functions are determined to give the Mayer bonds

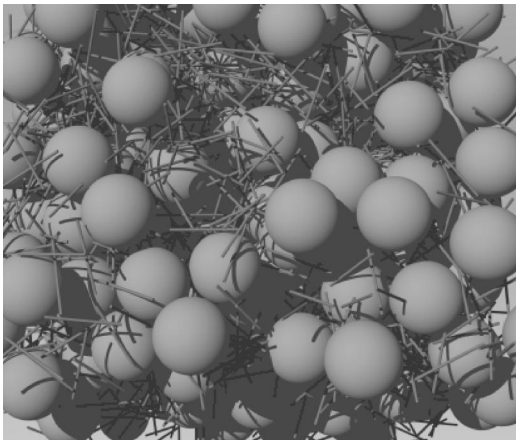

FIG. 1. Snapshot from simulation of the rod-sphere mixture at $L=\sigma$, $\eta=0.3$, $\rho_N=8\rho_S$ (statepoint II in Fig. 2). The rods are rendered with a finite diameter of 0.02σ.

$f_{ij}=\exp(V_{ij})-1$ by a linear combination of terms $w^i_\gamma(\mathbf{r}')\bigcirc w^j_{3-\gamma}(\mathbf{r}'')$, where $g(\mathbf{r}')\bigcirc h(\mathbf{r}'')=\int \mathrm{d}^3x\, g(\mathbf{x})h(\mathbf{r}-\mathbf{x})$. For needles, we follow Ref. [11] to obtain

$$w_1^N(\mathbf{r},\mathbf{\Omega})=\tfrac{1}{4}\int_{-L/2}^{L/2}\mathrm{d}l\;\delta(\mathbf{r}+\mathbf{\Omega}l), \tag{1}$$

$$w_0^N(\mathbf{r},\mathbf{\Omega})=\frac{1}{2}[\,\delta(\mathbf{r}+\mathbf{\Omega}L/2)+\delta(\mathbf{r}-\mathbf{\Omega}L/2)], \tag{2}$$

where $\delta(r)$ is the Dirac distribution, $\mathbf{\Omega}$ is a unit vector pointing along the needle axis, and $\mathbf{r}$ is the spatial coordinate. The function w_1^N describes the linear extent of a needle [15], whereas w_0^N is characteristic of its endpoints. For infinitely thin needles, both surface and volume vanish, and so should the corresponding weights, $w_2^N=w_3^N=0$. Indeed, as will be seen *a posteriori*, such terms are not needed to construct the DFT. For spheres, the usual weight functions [10,12] are

$$w_3^S(\mathbf{r})=\theta(R-r),\quad w_2^S(\mathbf{r})=\delta(R-r), \tag{3}$$

$$\mathbf{w}_{v2}^S(\mathbf{r})=w_2^S(\mathbf{r})\mathbf{r}/r,\quad \hat{\mathbf{w}}_{m2}^S(\mathbf{r})=w_2^S(\mathbf{r})[\,\mathbf{rr}/r^2-\hat{\mathbf{1}}/3], \tag{4}$$

where $r=|\mathbf{r}|$, $\theta(r)$ is the step function, and $\hat{\mathbf{1}}$ is the identity matrix. Further, linearly dependent, weights are $w_1^S(\mathbf{r})=w_2^S(\mathbf{r})/(4\pi R), \mathbf{w}_{v1}^S(\mathbf{r})=\mathbf{w}_{v2}^S(\mathbf{r})/(4\pi R), w_0^S(\mathbf{r})=w_1^S(\mathbf{r})/R$. The weight functions for spheres have different tensorial rank: w_0^S, w_1^S, w_2^S, and w_3^S are scalars; $\mathbf{w}_{v1}^S$ and $\mathbf{w}_{v2}^S$ are vectors; and $\hat{\mathbf{w}}_{m2}^S$ is a (traceless) matrix. These functions give the Mayer bond between pairs of spheres [10] through $-f_{SS}/2=w_3^S\circ w_0^S+w_2^S Z\circ w_1^S-\mathbf{w}_{v2}^S\circ\mathbf{w}_{v1}^S$. However, they are not sufficient to recover the sphere-needle Mayer bond [11]. This is achieved through

$$w_2^{SN}(\mathbf{r},\mathbf{\Omega})=2|\mathbf{w}_{v2}^S(\mathbf{r})\cdot\mathbf{\Omega}|, \tag{5}$$

which contains information about *both* species: it is nonvanishing on the surface of a sphere with radius R, but this surface is ''decorated'' with an $\mathbf{\Omega}$-dependence. Loosely speaking, w_2^{SN} describes how a sphere looks from the viewpoint of a rod. Technically, it generates the Mayer bond through $-f_{SN}(\mathbf{r},\mathbf{\Omega})=w_3^S(\mathbf{r}')\bigcirc w_0^N(\mathbf{r}'',\mathbf{\Omega})+w_2^{SN}(\mathbf{r}',\mathbf{\Omega})\bigcirc w_1^N(\mathbf{r}'',\mathbf{\Omega})$, where $\mathbf{r}$ is the difference vector between sphere and needle position. The weight functions are used to smooth the possibly highly inhomogeneous density profiles by convolutions,

$$n_\nu^N(\mathbf{r},\mathbf{\Omega})=\rho_N(\mathbf{r}',\mathbf{\Omega})\bigcirc w_\nu^N(\mathbf{r}'',\mathbf{\Omega}), \tag{6}$$

$$n_\nu^S(\mathbf{r})=\rho_S(\mathbf{r}')\bigcirc w_\nu^S(\mathbf{r}''), \tag{7}$$

$$n_2^{SN}(\mathbf{r},\mathbf{\Omega})=\rho_S(\mathbf{r}')\bigcirc w_2^{SN}(\mathbf{r}'',\mathbf{\Omega}), \tag{8}$$

where $\rho_S(\mathbf{r}')$, and $\rho_N(\mathbf{r}',\mathbf{\Omega})$ are the one-body density distributions of spheres and needles, respectively. Note that n_ν^N and n_ν^S are ''pure'' weighted densities, involving only variables of either species [10,11]. In contrast, our n_2^{SN} is a convolution of the sphere density with an orientation-dependent weight function; hence, it combines characteristics of both species.

Finally, the (Helmholtz) excess free energy is obtained by integrating over a free energy density,

$$F_{\mathrm{exc}}[\rho_S,\rho_N]=k_BT\int\mathrm{d}^3x\int\frac{\mathrm{d}^2\Omega}{4\pi}\Phi(\{n_\gamma^i\}), \tag{9}$$

where k_B is Boltzmann's constant, T is temperature, and the (local) reduced free energy density Φ is a simple function (not a functional) of the weighted densities n_γ^i. The variable $\mathbf{x}$ runs over space, as usual [10,11]. Here we allow Φ to depend on orientation, and hence integrate $\mathbf{\Omega}$ over the unit sphere. The functional form of Φ is obtained by consideration of the exact zero-dimensional ($0D$) excess free energy. For the present model this is identical to the AO case [17], namely, the statistics of η hard and η' ideal particles, and is given by $F_{0\mathrm{D}}/k_BT=(1-\eta-\eta')\ln(1-\eta)+\eta$ [17]. Considering multicavity distributions [12], we obtain $\Phi=\Phi_S+\Phi_{SN}$ with

$$\begin{aligned}\Phi_S=&-n_0^S\ln(1-n_3^S)+(n_1^Sn_2^S-\mathbf{n}_{v1}^S\cdot\mathbf{n}_{v2}^S)/(1-n_3^S)\\&+[(n_2^S)^3/3-n_2^S(\mathbf{n}_{v2}^S)^2+3(\mathbf{n}_{v2}^S\hat{\mathbf{n}}_{m2}^S\mathbf{n}_{v2}^S\\&-3\det\hat{\mathbf{n}}_{m2}^S)/2]/[8\pi(1-n_3^S)^2],\end{aligned} \tag{10}$$

which is equal to the pure HS case [10,12]. The contribution due to the presence of the needles is

$$\Phi_{SN}=-n_0^N\ln(1-n_3^S)+\frac{n_1^Nn_2^{SN}}{1-n_3^S}, \tag{11}$$

where the arguments are suppressed in the notation; see Eqs. (6)–(8). This completes the prescription for the functional.

We investigate some of the properties of the homogeneous, isotropic bulk mixture. In this case the weighted densities become proportional to the respective bulk densities, $n_\nu^i=\xi_\nu^i\rho_i$, where the proportionality constants are fundamental measures given by $\xi_\nu^i=\int\mathrm{d}^3x\,w_\nu^i$. For spheres ξ_3^S

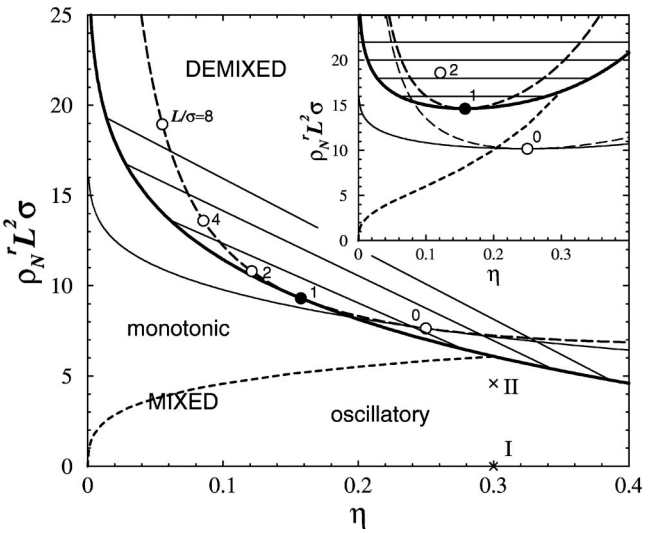

FIG. 2. Phase diagram of the rod-sphere mixture as a function of sphere density η and scaled needle density $\rho_N L^2\sigma$. Shown is the universal spinodal (dashed line). For $L/\sigma=1$ the binodal (thick line), tie lines (thin straight lines), Fisher-Widom line (dotted line), and statepoints I and II (crosses) are indicated. Circles represent the critical points for $L/\sigma=0,1,2,4$, and 8. The thin line is the metastable binodal for $L/\sigma=0$. Inset shows corresponding plots as a function of needle reservoir density $\rho_N^r L^2\sigma$. Note that there are now separate spinodals (dashed lines).

$=4\pi R^3/3, \xi_2^S=4\pi R^2, \xi_1^S=R, \xi_0^S=1$, whereas for needles $\xi_1^N=L/4, \xi_0^N=1$, and, there is also a combined fundamental measure $\xi_2^{SN}=4\pi R^2 (=\xi_2^S)$. Then the excess Helmholtz free energy per volume V is given by $F_{\rm exc}(\rho_S,\rho_N)/V=f_{\rm HS}(\rho_S)-\rho_N k_B T \ln\alpha(\rho_S)$, where $f_{\rm HS}(\rho_S)$ is the excess free energy density of pure hard spheres in the scaled-particle [Percus-Yevick (PY) compressibility] approximation and $\alpha=(1-\eta)\exp[-(3/2)(L/\sigma)\eta/(1-\eta)]$, which is identical to that of Ref. [7], leading to (sphere) gas-liquid phase separation [7,18]. As an explanatory case, we choose $L/\sigma=1$, and display the gas-liquid portion of the phase diagram as a function of η and $\rho_N L^2\sigma$ in Fig. 2. We find that in this representation the spinodals for all size ratios $s=L/\sigma$ collapse onto each other and are given analytically by $\rho_N^{\rm spin} L^2\sigma=8(1+2\eta)^2/(3\pi\eta)$. The critical point moves along this curve as a function of s (see Fig. 2 for $s=0,1,2,4$, and 8) and is given by [7] $\eta_{\rm crit}=(10+3s-3\sqrt{4+12s+s^2})/(16-12s)$. The Fisher-Widom line [19] divides the phase diagram into regions of different asymptotic decay of the free bulk pair correlations. Here the decay is damped oscillatory for small needle densities, where the packing of spheres dominates. It becomes monotonic upon increasing needle density; the ideality between needles washes out the oscillations. In the inset of Fig. 2 the dependence on the actual needle density in the system is replaced by that in a needle reservoir, in chemical equilibrium with the system, which is given here by $\rho_N^r=\alpha\rho_N$. The reservoir density plays a role similar to that of inverse temperature in simple systems, and the topology of the phase diagram resembles that of a simple substance. Demixing is preempted by freezing for $s\lesssim 0.3$, as shown by BF. However, if we trace the critical point inside the metastable region, we find that it smoothly approaches $\eta=1/4$, $\rho_N L^2\sigma=24/\pi$, $\rho_N^r L^2\sigma=32/\pi$ for $s\to 0$. This is in contrast to free volume theory for the AO model, where demixing is preempted by freezing at a similar size ratio [16], but with the (metastable) critical point shifting to high density, thereby crossing hard sphere fluid-solid coexistence. Whether this difference has implications for the existence of an isostructural solid-solid transition in the present model constitutes an interesting aspect.

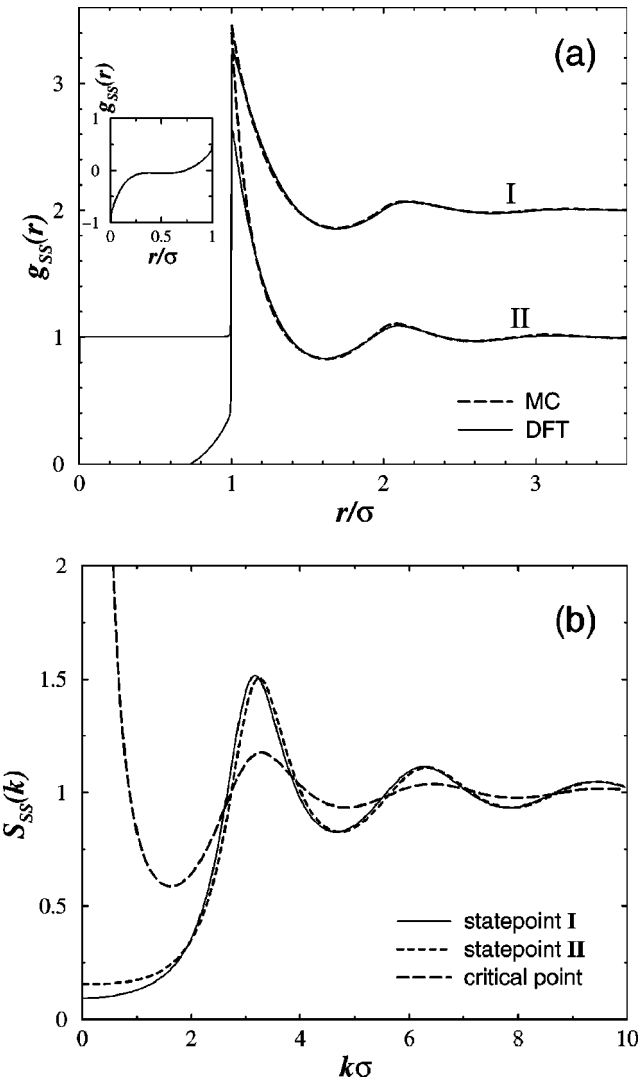

FIG. 3. Pair structure for spheres as obtained from DFT at $L/\sigma=1$, $\eta=0.3$, $\rho_N=0$ (statepoint I) and $\rho_N=4.58\,366/L^2\sigma$ (statepoint II). (a) Partial sphere-sphere pair correlation function compared to MC simulation. Results for statepoint I are shifted upwards by one unit for clarity. The inset shows the DFT result inside the core for statepoint II. (b) Corresponding partial structure factor at statepoints I and II, as well as at the gas-liquid critical point.

Next we investigate the bulk pair structure. The pair direct correlation functions are obtained as $c_{ij}=-(k_B T)^{-1}\delta^2 F_{\rm exc}/\delta\rho_i\delta\rho_j$. Due to their geometric representation as convolutions of single particle functions, the c_{ij} vanish beyond the range of interaction, similar to what is found in PY. The Ornstein-Zernike (OZ) relations then yield partial structure factors and pair correlation functions. In or-

der to test the accuracy of the theoretical results, we have carried out canonical Monte Carlo (MC) computer simulations with 256 spheres and up to 2048 needles; for the pair correlations, 10^5 moves per particle were performed. Here we focus on the correlations $g_{SS}(r)$ between spheres. Figure 3(a) shows results for $L/\sigma=1$, $\eta=0.3$, and two different needle densities, $\rho_N=0$ (statepoint I, depicted in the phase diagram Fig. 2), and $\rho_N=8\rho_S=4.58\,366/L^2\sigma$ (statepoint II). In the absence of needles (statepoint I) the DFT result reproduces the rather accurate PY solution for hard spheres. Increasing the needle density (statepoint II, where the snapshot, Fig. 1, is taken) leads to an increase of the contact value; the period of oscillations becomes shorter, hence the spheres tend to be at smaller separation. The DFT provides a good description of the MC results, except for an underestimation of the contact value and nonzero values inside the core. This could be remedied by using the test-particle limit, i.e. minimizing the grand potential in the presence of a sphere fixed at the origin. The corresponding structure factors $S_{SS}(k)$ are shown in Fig. 3(b). Adding needles (statepoint II) leads to a small shift towards larger k-values, as well as to an increase in $S_{SS}(0)$. In addition, we plot $S_{SS}(k)$ at the critical point obtained from the free energy; $S_{SS}(k\rightarrow 0)$ divergesconsistently.

Let us conclude with two remarks. First, in view of the successful treatment of the bulk, the present theory offers direct access to a wide range of interesting interfacial and confined situations, such as wetting, layering transitions, and capillary condensation, as well as the study of the free interface between demixed fluid phases. Especially appealing is the perspective to investigate the degree of universality of the entropic wetting scenario in the AO model [20], found recently by a similar DFT treatment [17]. For the current model, interesting orientational behavior of the rods may be anticipated: For example, at the free (gas-liquid) interface between demixed phases, the rod orientations will in general show a tendency to order, although the distributions are isotropic in both bulk phases. Second, the crucial extensions of geometry-based DFT done in this work are the integration over director space [Eq. (9)], and the introduction of double-indexed weight functions [Eq. (5)]. Whether these technical tools permit the treatment of other rotating hard bodies constitutes an important point for future investigations.

I thank Bob Evans and Holger Harreis for valuable remarks, and Gerrit Vliegenthart and Arjun Yodh for stimulating discussions.

[1] See e.g., M. Dijkstra, R. van Roij, and R. Evans, Phys. Rev. Lett. **81**, 2268 (1998); **82**, 117 (1999).
[2] S. Asakura and F. Oosawa, J. Chem. Phys. **22**, 1255 (1954); see also A. Vrij, Pure Appl. Chem. **48**, 471 (1976).
[3] G. A. Vliegenthart and H. N. W. Lekkerkerker, J. Chem. Phys. **111**, 4153 (1999).
[4] G. H. Koenderink *et al.*, Langmuir **15**, 4693 (1999).
[5] Y. Mao, M. E. Cates, and H. N. W. Lekkerkerker, Phys. Rev. Lett. **75**, 4548 (1995); J. Chem. Phys. **106**, 3721 (1997).
[6] K. Yaman, C. Jeppesen, and C. M. Marques, Europhys. Lett. **42**, 221 (1998).
[7] P. Bolhuis and D. Frenkel, J. Chem. Phys. **101**, 9869 (1994).
[8] H. N. W. Lekkerkerker *et al.*, Europhys. Lett. **20**, 559 (1992).
[9] R. Evans, in *Fundamentals of Inhomogeneous Fluids*, edited by D. Henderson (Dekker, New York, 1992), p. 85.
[10] Y. Rosenfeld, Phys. Rev. Lett. **63**, 980 (1989).
[11] Y. Rosenfeld, Phys. Rev. E **50**, R3318 (1994).
[12] P. Tarazona, Phys. Rev. Lett. **84**, 694 (2000).
[13] J. A. Cuesta, Phys. Rev. Lett. **76**, 3742 (1996).
[14] A. Chamoux and A. Perera, J. Chem. Phys. **104**, 1493 (1996).
[15] Using $\mathbf{r}=(r_\parallel,r_{\perp 1},r_{\perp 2})$, where $r_\parallel$ is parallel, and $r_{\perp 1},r_{\perp 2}$ are perpendicular to $\mathbf{\Omega}$, respectively, one obtains $w_1^N(\mathbf{r},\mathbf{\Omega})=\delta(r_{\perp 1})\delta(r_{\perp 2})$ if $|r_\parallel|<L/2$, and zero else.
[16] J. M. Brader, M. Dijkstra, and R. Evans, J. Phys.: Condens. Matter **11**, 10 079 (1999).
[17] M. Schmidt, H. Löwen, J. M. Brader, and R. Evans, Phys. Rev. Lett. **85**, 1934 (2000).
[18] In Ref. [7] the Carnahan-Starling equation of state for hard spheres was used.
[19] R. Evans *et al.*, J. Chem. Phys. **100**, 591 (1994).
[20] J. M. Brader, R. Evans, M. Schmidt, and H. Löwen (unpublished).